Earth and Planetary Science Letters 289 (2010) 449–456

Contents lists available at ScienceDirect

Earth and Planetary Science Letters

journal homepage: www.elsevier.com/locate/epsl

Determination of the high-pressure properties of fayalite from first-principles calculations

Stephen Stackhouse [a,*], Lars Stixrude [b], Bijaya B. Karki [c]

[a] Department of Geological Sciences, University of Michigan, 1100 North University Ave., Ann Arbor, Michigan, 48109-1005, USA
[b] Department of Earth Sciences, University College London, Gower Street, London WC1E 6BT, UK
[c] Department of Computer Science, Louisiana State University, 283 Coates Hall, Baton Rouge, LA 70803, USA

ARTICLE INFO

Article history:
Received 6 June 2009
Received in revised form 17 November 2009
Accepted 18 November 2009

Editor: R.D. van der Hilst

Keywords:
first-principles
ab initio
GGA+*U*
fayalite
high-pressure
elastic properties

ABSTRACT

We have calculated the high-pressure properties of fayalite, including band structure, magnetism, equation-of-state and elastic properties using density functional theory within the generalized gradient approximation (GGA) and using the GGA + *U* method. We show for the first time that the addition of an on-site Hubbard repulsion term to the GGA leads to improved agreement between calculated and experimental values of structural and elastic properties, as well as electronic band gap, particularly at high pressure. High-pressure elastic instability, originating in the vanishing of the elastic constant c_{44} and previously predicted on the basis of extrapolated experimental data, is found with the GGA + *U* method. Experimental measurements of the elastic constants agree better with the GGA + *U* method, than with the GGA, which calls for a reassessment of the structural and elastic properties of iron-bearing minerals calculated using standard density functional theory, which have hitherto been used to interpret the structure and dynamics of the mantle. The improvement can be related to the better description of magnetic structure: without the Hubbard *U* the magnetic moments on the iron ions decrease with pressure, whereas when it is included they remain almost constant, at least, up to the highest pressure studied. This also leads to better predictions of equation-of-state. Our calculated partial density-of-states indicate that the lowest energy excitation across the electronic band gap lies within the *d*-orbital manifold, and we argue that this is not observed at ambient pressure because the signal in the optical spectrum is too weak, accounting for apparent discrepancies with reported experimental values. Upon compression the nature of the gap changes due to the broadening of the 3*d* manifold, and this likely renders the fundamental gap observable in optical spectroscopy at high pressure, accounting for the better agreement between theory and experiment above 20 GPa. We associate the changes in the character of the bands with a change in the crystal structure.

1. Introduction

Fayalite is the pure iron end-member of olivine, thought to be the most abundant phase in the Earth's upper mantle (Ringwood, 1970). Olivine is expected to predominate from the base of the crust to the 410 km seismic discontinuity and may be preserved (in a metastable state) to greater depths in subducting slabs (Green and Burnley, 1989; Wu et al., 1993). It is important to understand the influence of iron on the properties of olivine, because of its unusual characteristics as compared with the other major cations, including its large mass and electronic structure dominated by *d*-states. These lead to it having a pronounced effect on density, elastic wave velocities and electrical conductivity and thus, in turn, on mantle dynamics and the interpretation of geophysical observations.

The high pressure behavior of fayalite allows us to explore two important issues. The first of these is the behavior of silicates as they are compressed outside their thermodynamic stability field. While the thermodynamic stability field of olivine is well known (Yagi et al., 1987), its behavior under metastable over-compression, as would occur in a kinetically hindered subducting slab is still not well understood. Pressure-induced amorphization of silicates is often observed (Richet and Gillet, 1997) and in some cases may be related to a dynamical instability of the lattice (Kingma et al., 1993). Based on extrapolation of experimental data, it has been proposed that an elastic instability occurs in fayalite at about 35 GPa (Speziale et al., 2004), and this could be related to the observed amorphization transition (Williams et al., 1990; Richard and Richet, 1990; Andrault et al., 1995). The second relevant issue concerns the nature of the insulator to metal transition in silicates. Iron-free silicates have large band gaps that apparently do not close until pressures well beyond those at the center of the Earth (Umemoto et al., 2006), but iron-

* Corresponding author. Present address: Department of Earth and Planetary Science, University of California, Berkeley, 307 McCone Hall, Berkeley, CA 94720-4767, USA. Tel.: +1 510 642 7030; fax: +1 510 643 9980.
E-mail addresses: sstackho@umich.edu (S. Stackhouse), l.stixrude@ucl.ac.uk (L. Stixrude), karki@csc.lsu.edu (B.B. Karki).

0012-821X/$ – see front matter © 2009 Elsevier B.V. All rights reserved.
doi:10.1016/j.epsl.2009.11.033

bearing silicates have much smaller band gaps that may be influenced by the spin state of the iron cation (Badro et al., 2004). Experimental studies suggest that the band gap of fayalite narrows under static compression at low temperature (Williams et al., 1990), a phenomenon that could be related to the simultaneous observation of pressure-induced amorphization.

We also consider fayalite an ideal testing ground for ab initio theory. Density functional theory (DFT) (Hohenberg and Kohn, 1964; Kohn and Sham, 1965) has been applied with much success to the study of a wide range of mantle minerals (Karki et al., 2001; Brodholt and Vočadlo, 2006), but studies of iron-bearing phases have been limited. This is because transition metal oxides such as fayalite present a particular challenge to the method, due to the strong correlation of electrons in the *d*-states. This correlation is responsible for magnetism and insulating behavior in these systems and its effects are not fully accounted for in the most widely used approximations: the local density approximation (LDA) and generalized gradient approximation (GGA). In view of this, density functional theory can fail to predict the correct band structure of iron-bearing minerals, such as iron oxide (Isaak et al., 1993a; Alfredsson et al., 2004) and fayalite (Cococcioni et al., 2003; Jiang and Guo, 2004). In spite of this, it has continued to be used to predict the elastic properties of iron-bearing phases, such as silicate perovskite and post-perovskite (e.g. Kiefer et al., 2002; Li et al., 2005; Caracas and Cohen, 2005; Tsuchiya and Tsuchiya, 2006; Stackhouse et al., 2006), on the assumption that they are less affected. However this is unknown, since no corresponding experimental data exists with which to compare. In contrast, abundant experimental data exists for fayalite (Sumino, 1979; Graham et al., 1988; Wang et al., 1989; Isaak et al., 1993b; Speziale et al., 2004), providing the possibility to assess the accuracy of the method.

In the present work we also investigate an advanced method, referred to as GGA $+U$, whereby strong correlation is captured via an additional local Hubbard repulsion of magnitude U (Anisimov et al., 1991, 1997). This approach can lead to improved predictions of crystal structure, band gaps, and magnetic properties (Gramsch et al., 2003; Jiang and Guo, 2004; Alfredsson et al., 2004; Cococcioni and de Gironcoli, 2005). However little is known about the influence of U on elastic properties. One study found a small effect, although in a system for which there is, yet again, no corresponding experimental data (Stackhouse and Brodholt, 2008).

2. Theory

Our calculations were performed using the projector-augmented-wave implementation (Blöchl, 1994; Kresse and Joubert, 1999) of the density functional theory based VASP code (Kresse and Furthmüller, 1996a,b), which incorporates a simplified GGA $+U$ scheme (Dudarev et al., 1998). The exchange-correlation functional adhered to the PBE form of the generalized gradient approximation (GGA) (Perdew et al., 1996) and the potentials were generated using the following electronic configurations: $3p^6\ 3d^7\ 4\ s^1$ for iron, $3\ s^2\ 3p^2$ for silicon and $2\ s^2\ 2p^4$ for oxygen. For all calculations the kinetic-energy cut-off for the plane-wave expansion was 800 eV, the Brillouin zone sampled using a $4 \cdot 2 \cdot 4$ special k-point grid (Monkhorst and Pack, 1976) and the convergence criteria for structural optimization was 10^{-6} eV. For both the GGA and GGA $+U$ calculations we applied Fermi (i.e., physical) smearing (Mermin, 1965) with a broadening width of 0.2 eV, except for calculation of the electronic density-of-states when the tetrahedron smearing method with Blöchl corrections (Blöchl et al., 1994) was used. These settings ensured that calculated total energies were converged to less than one meV per atom and elastic constants to within about one percent. For further information on density functional theory and its application to mineral physics, the reader is directed to a review (Stixrude et al., 1998).

The GGA $+U$ method requires specification of an onsite exchange interaction parameter J and onsite Coulomb interaction parameter U. However in the most widely used implementation employed in the present work (Dudarev et al., 1998), the results depend only on the difference between these values. It is therefore common to define an effective U parameter $U_{\mathrm{eff}} = U - J$ and refer to U_{eff} as simply U, which is the notation adopted here. Self-consistent calculations indicate that for fayalite U should be about 4.6 eV and 4.9 eV for the two distinct iron sites (Cococcioni et al., 2003; Cococcioni and de Gironcoli, 2005). In view of this, we used $U = 4.8$ eV. We also explored a range of alternative values of U, between 1.0 eV and 6.0 eV.

In all our calculations we assumed a ferromagnetic state of order and allowed the magnitude of the moment to vary. Fayalite is known to be a non-co-linear anti-ferromagnet at low temperature with a Néel temperature of 65 K at ambient pressure, rising to 100 K at 16 GPa (Hayashi et al., 1987). But at room temperature and above, the regime of primary interest in geophysics and the comparison with high-pressure experimental data, the moments are disordered. Since non-co-linear calculations are more challenging and as the magnetic state at high pressure is poorly known, ferromagnetic order seems a good first order assumption. In addition, previous studies have shown that nature of the magnetic order has only very subtle effects on crystal structure (Cococcioni et al., 2003; Jiang and Guo, 2004).

At each volume considered, the structure was optimized allowing all cell parameters and atomic positions to vary. Because of our particular interest in mechanical instability, we took the unusual step of leaving the symmetry unconstrained (*P* 1), increasing the computational expense of the calculations considerably. Previous studies have shown that electronic spin transitions can be associated with symmetry breaking, with important consequences for predicted spin transition pressures (Bengtson et al., 2008). Despite this extra freedom, we find that the olivine structure was preserved during relaxation at all volumes, except for the smallest volume in the GGA calculations. To determine the athermal elastic constants three different orthorhombic and one triclinic strains of magnitude $\pm 0.5\%$ were applied to the optimized models, and the atomic positions allowed to fully relax in the strained configurations (Karki et al., 2001). Then a second-order polynomial was fit to the relationship between applied strain and induced, calculated stress.

In order to compare with experiment, the resulting athermal values were converted to room-temperature adiabatic values making use of the thermodynamic identity:

$$\left(\frac{dc_{ij}}{dT}\right)_V = \left(\frac{dc_{ij}}{dT}\right)_P + \left(\frac{dP}{dT}\right)_V \left(\frac{dc_{ij}}{dP}\right)_T \tag{1}$$

with values for the temperature derivatives of the elastic constants at constant pressure taken from Isaak et al. (1993b), that for the isochoric change in pressure with temperature from Anderson and Isaak (1995) and those for the pressure derivatives of the elastic constants at constant temperature from Speziale et al. (2004). Bulk and shear moduli were computed as the Voigt-Reuss-Hill average (Hill, 1963).

To correct our athermal calculations for the influence of phonon excitation and the well known under-binding tendency of the GGA, we report pressures as:

$$P(V,T) = P_{VASP}(V,0K) + P_{EMP} + P_{ZPM}(V) + P_{TH}(V,T) \tag{2}$$

where P is the total pressure, $P_{VASP}(V, 0K)$ the (athermal) pressure calculated by the VASP code at volume V and 0 K; P_{EMP} a volume- and temperature-independent empirical pressure correction; $P_{ZPM}(V)$ the pressure associated with zero-point motion and $P_{TH}(V, T)$ the thermal pressure at volume V and temperature T (de Koker et al., 2008). The empirical pressure correction P_{EMP} was calculated as:

$$P_{EMP} = -P_{VASP}(V_{EXP}) \tag{3}$$

where V_{EXP} is the experimental volume at zero pressure and static conditions computed using the thermodynamic model of Xu et al. (2008). Values for $P_{ZPM}(V)$ and $P_{TH}(V, T)$ were also computed using the thermodynamic model of Xu et al. (2008). The calculated value of P_{EMP} for the GGA was -2.87 GPa. For the GGA $+U$ method it was -5.36 GPa with $U = 2.0$ eV and -6.72 GPa with $U = 4.8$ eV. These lie within the

range of pressure corrections calculated in previous investigations (*e.g* $P_{EMP} = -12.08$ GPa for $MgSiO_3$ perovskite using the GGA (Oganov et al., 2001) and $P_{EMP} = +1.6$ GPa for forsterite using the LDA (de Koker et al., 2008)) and consistent with a host of other studies of silicates that find that the LDA generally slightly overbinds and the GGA underbinds by a larger amount.

3. Results

The calculated equation-of-state and lattice parameters of fayalite are in good agreement with experimental values at low pressures, irrespective of whether they were calculated with the GGA or GGA $+U$ method and the value of U used (Figs. 1 and 2; Table 1). The ambient pressure lattice parameters calculated using the GGA $+U$ method vary less than a percent as U varies from 1 eV to 6 eV. The maximum difference between the lattice parameters calculated with the GGA and those of Fujino et al. (1980) is 1.70%, while the GGA $+U$ method does a little better, with a maximum difference of 0.30% with $U = 2.0$ eV and 0.49% with $U = 4.8$ eV. Though it is significant that the GGA and GGA $+U$ method both accurately predict the correct shape of the unit cell (i.e., c/a and b/a ratios), especially as the structure is highly elastically anisotropic, the good agreement in the zero pressure volume is due to the application of the empirical pressure correction (Eq. (3)). This correction is larger for the GGA $+U$ pressures than the GGA pressures, which means that the well-known under-binding tendency of the GGA is somewhat exacerbated by the addition of U.

The situation is quite different at high pressures where the lattice parameters and equation-of-state calculated using the GGA and GGA $+U$ method diverge. The GGA predicts lattice parameters and an equation-of-state that differ from experimental values at high pressures. In particular, the GGA predicts an equation-of-state that is much too soft. In contrast, the two sets of GGA $+U$ values are in good agreement with experimental values and each other at nearly all pressures. In particular, the GGA $+U$ values agree with experiment to within experimental uncertainty, except for the highest pressure volume measurements of Andrault et al. (1995) and the highest pressure measurements of the b axis of Williams et al. (1990). However it is likely that these high-pressure experimental data are biased by non-hydrostaticity (Speziale et al., 2004).

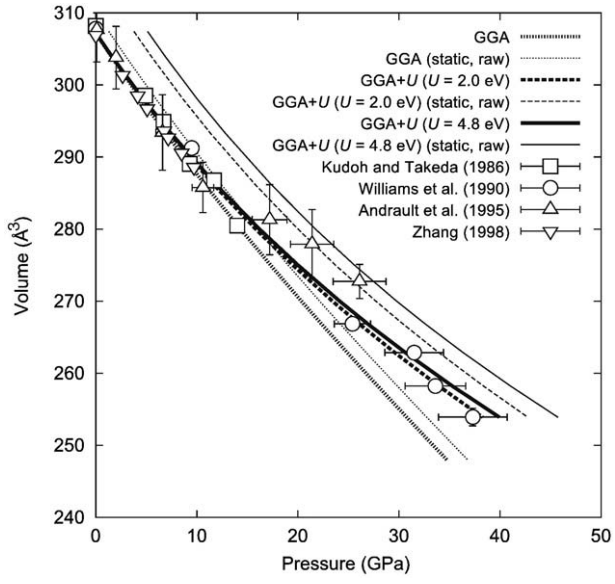

Fig. 1. Equation-of-state of fayalite calculated using the GGA and GGA $+U$ method, with $U = 2.0$ eV or 4.8 eV, and corresponding experimental data. Note that, Kudoh and Takeda (1986) studied an $(Fe_{0.920}Mn_{0.055}Mg_{0.020}Si_{0.005})_2SiO_4$ composition; Williams et al. studied an Fe_2SiO_4 composition; Andrault et al. (1995) studied an $(Fe_{0.99}Mn_{0.01})_2SiO_4$ composition; and Zhang (1998) studied an Fe_2SiO_4 composition. The GGA and GGA $+U$ results are plotted using both the raw, static and corrected pressure and were fit to a third-order Birch–Murnaghan equation-of-state (Birch, 1947). Using the corrected pressure the equation-of-state parameters are: GGA [$V_0 = 76.8$ Å^3, $K_0 = 145$ GPa, and $K_0' = 1.7$]; GGA $+U$ ($U = 2.0$ eV) [$V_0 = 76.8$ Å^3, $K_0 = 146$ GPa, and $K_0' = 3.4$] and GGA $+U$ ($U = 4.8$ eV) [$V_0 = 76.8$ Å^3, $K_0 = 147$ GPa, and $K_0' = 3.7$].

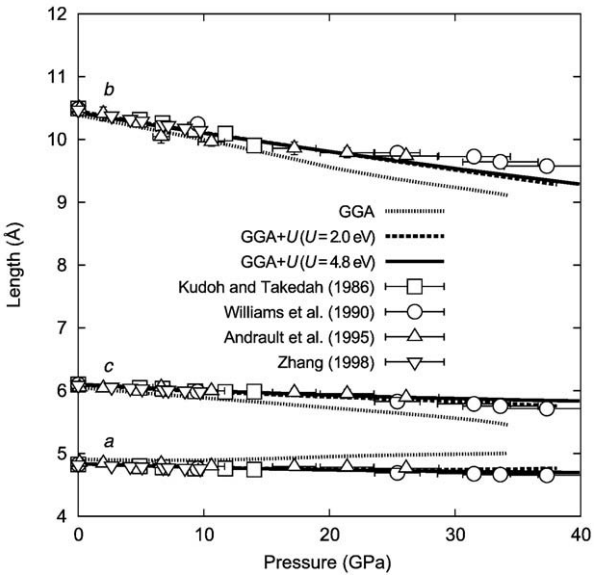

Fig. 2. Lattice parameters of fayalite as a function of pressure, calculated using the GGA and GGA $+U$ method, with $U = 2.0$ eV and 4.8 eV, and corresponding experimental data. Note that, Kudoh and Takeda (1986) studied an $(Fe_{0.920}Mn_{0.055}Mg_{0.020}Si_{0.005})_2SiO_4$ composition; Williams et al. studied an Fe_2SiO_4 composition; Andrault et al. (1995) studied an $(Fe_{0.99}Mn_{0.01})_2SiO_4$ composition; and Zhang (1998) studied an Fe_2SiO_4 composition.

The calculated ambient pressure elastic constants of fayalite depend a great deal on the value of U used (Fig. 3). The elastic constants increase with increasing U at fixed volume, except for the off-diagonal elastic constants (c_{12}, c_{13}, c_{23}), which change little with increasing U. Best agreement with the experimental values, listed in Table 1, is found with $U = 2.0$ eV (Table 2). Using this value the largest discrepancies are in the off-diagonal elastic constants (close to 20%). The other elastic constants agree to within an average of 6%. The predicted Voigt-Reuss-Hill bulk modulus is 10% higher than the average experimental value, while the Voigt-Reuss-Hill shear modulus is almost identical.

Table 1
Density, volume and lattice constants of fayalite at ambient conditions.

		U (eV)	ρ (g cm^{-3})	V (Å^3)	a (Å)	b (Å)	c (Å)
Theoretical values							
This work [a]	GGA	0.0	4.402	307.424	4.901	10.379	6.043
This work [a]	GGA $+U$	2.0	4.402	307.424	4.834	10.450	6.086
This work [a]	GGA $+U$	4.8	4.402	307.424	4.834	10.428	6.099
Cococcioni et al., 2003 [b]	LDA	–	4.765	284.054	4.757	10.176	5.868
Cococcioni et al., 2003 [c]	LDA	–	4.904	276.027	4.985	9.716	5.699
Cococcioni et al. 2003 [b]	GGA	–	4.339	311.912	4.874	10.562	6.059
Cococcioni et al. 2003 [c]	GGA	–	4.370	309.710	4.953	10.467	5.974
Jiang and Guo, 2004 [c]	GGA	–	4.443	304.666	4.956	10.337	5.947
Jiang and Guo, 2004 [c]	GGA $+U$	3.6	4.383	308.849	4.878	10.354	6.115
Experimental values							
Fujino et al. 1980			4.402	307.424	4.820	10.479	6.087

[a] Ferromagnetic configuration — unit cell optimized at fixed volume.
[b] Antiferromagnetic configuration 1.
[c] Antiferromagnetic configuration 2.

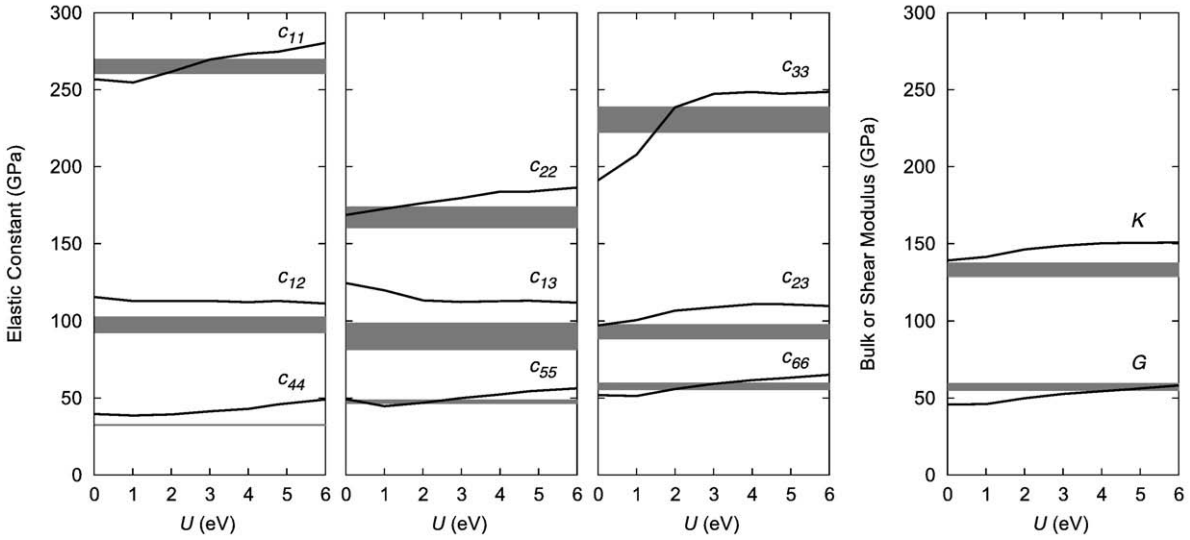

Fig. 3. Elastic constants and bulk and shear moduli of fayalite calculated using the GGA + *U* method, as a function of *U* value. GGA values correspond to *U* = 0.0 eV. The shaded bands represent the range of experimental values listed in Table 2.

The pressure dependencies of the elastic constants predicted with the GGA + *U* method show good agreement with experimental data with both values of *U* used, with the possible exception of c_{22} (Fig. 4). In particular, the large negative curvature in the pressure dependence of c_{44} is reproduced. Fayalite shows an elastic instability at high pressure using both the GGA and GGA + *U* method. The GGA calculations converge poorly as the instability is approached and the precise location or nature of the instability is not easy to determine. The poor convergence using the GGA is also responsible for the rapid oscillations in the values of the elastic constants with increasing pressure as the instability is approached. In the case of the GGA + *U* calculations the instability is well identified and is manifested in a vanishing of c_{44}, predicted to occur at 38 GPa with *U* = 2.0 eV and about 58 GPa with *U* = 4.8 eV. Experimental investigations report pressure-induced amorphization of fayalite at about 40 GPa, (Williams et al., 1990; Richard and Richet, 1990; Andrault et al., 1995), which is suggested to be a result of the vanishing of c_{44}. If amorphization is caused by the elastic instability, this comparison indicates again that a value of *U* = 2.0 eV leads to the best description of elastic properties.

We find that fayalite is a metal within the GGA, but that a finite band gap opens for finite values of *U* using the GGA + *U* method. The gap increases from 0.14 eV for *U* = 1.0 eV to 3.03 eV for *U* = 6 eV. These results are in reasonable accord with the results of previous investigations (Jiang and Guo, 2004; Cococcioni and de Gironcoli, 2005), with the respective values of the gap found in these studies being a little lower and a little higher than we find for the same values of *U*. We attribute these differences to the details of the calculations: different sets of pseudopotentials were used in the previous studies, versus the in-principle more accurate projector-augmented-wave method used in the present work. Magnetic structure apparently has little influence on the gap as the two previous studies assumed a co-linear anti-ferromagnetic spin arrangement.

Our GGA + *U* calculations indicate that fayalite remains an insulator over the entire pressure range considered in our investigation (Fig. 5), in agreement with experiment (Mao and Bell, 1972; Williams et al., 1990). For *U* = 2.0 eV, the band gap decreases from 0.85 eV at 0 GPa to 0.35 eV at 38 GPa, while for *U* = 4.8 eV the band gap decreases from 2.52 eV at 0 GPa to 2.24 eV at 40 GPa. These values lie about 1 eV below and above the reported experimental values respectively, suggesting that using a value of *U* = 3.5 eV would lead to an optimum description of the band gap. Previous theoretical results have also found that the band gap decreases but remains finite upon compression up to 25 GPa (Jiang and Guo, 2004).

The evolution of the band gap in our calculations is very different from that observed experimentally. In order to explore the origin of this difference further, we have computed the partial densities-of-

Table 2
Elastic constants and bulk and shear moduli of fayalite at ambient conditions (in GPa).

		U (eV)	c_{11}	c_{22}	c_{33}	c_{12}	c_{13}	c_{23}	c_{44}	c_{55}	c_{66}	*K*	*G*
Theoretical values													
This work [a]	GGA	0.0	257	169	191	116	125	97	40	49	52	139	46
This work [a]	GGA + *U*	2.0	262	176	238	113	113	107	39	47	56	147	50
This work [a]	GGA + *U*	4.8	275	184	247	113	113	111	46	54	63	151	56
Experimental values													
Sumino, 1979[b]			267	174	239	95	99	98	32	48	57	138	51
Graham et al., 1988[c]			267	160	222	92	81	88	32	47	57	129	50
Wang et al., 1989[d]			260	168	234	94	93	89	33	46	55	132	50
Isaak et al. (1993b)[e]			269	172	233	94	97	94	32	47	57	136	51
Speziale et al., 2004[f]			270	171	234	103	97	93	33	49	60	138	52

[a] Ferromagnetic configuration.
[b] Rectangular parallelepiped resonance technique — values as reported by Isaak et al., 1993b.
[c] Superposition ultrasonic interferometry method — samples contained trace amounts of MnO.
[d] Brillouin scattering — $(Fe_{0.95}Mn_{0.05})SiO_4$ composition.
[e] Rectangular parallelepiped resonance technique — samples contained trace amounts of MnO.
[f] Brillouin scattering — $(Fe_{0.94}Mn_{0.06})SiO_4$ composition.

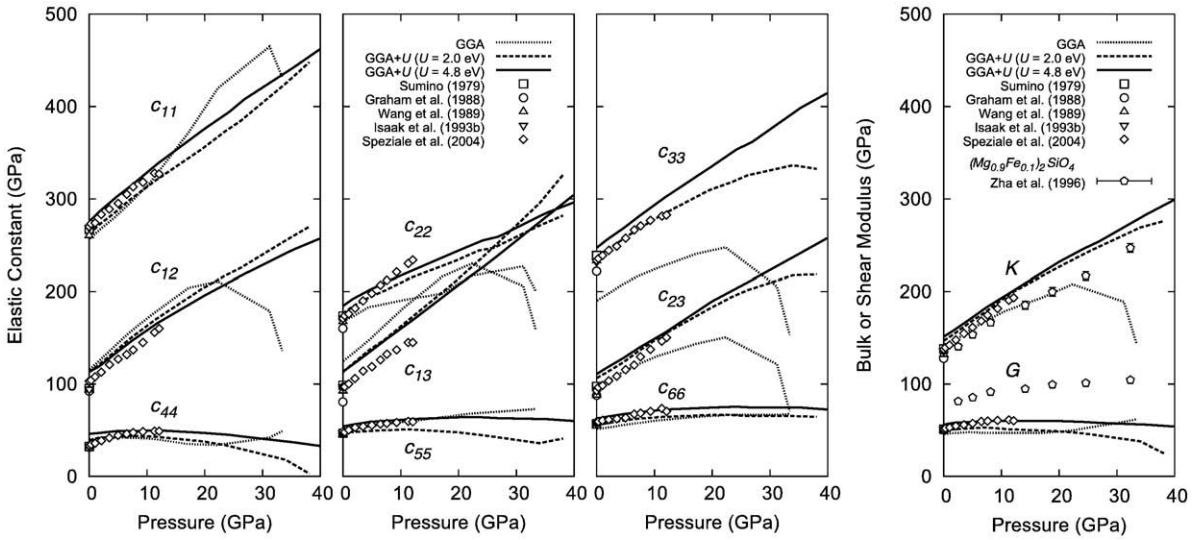

Fig. 4. Elastic constants and bulk and shear moduli of fayalite calculated using the GGA and GGA + U method, with $U = 2.0$ eV and 4.8 eV, and corresponding experimental data. Note that, Sumino (1979) studied an Fe_2SiO_4 composition; the sample of Graham et al. (1988) contained traces of MnO; Wang et al. (1989) studied an $(Fe_{0.95}Mn_{0.05})_2SiO_4$ composition; Isaak et al. (1993b) studied an Fe2SiO4 composition; and Speziale et al. (2004) studied an $(Fe_{0.94}Mn_{0.06})_2SiO_4$ composition. Experimental values for the bulk and shear moduli of olivine with an $(Mg_{0.9}Fe_{0.1})_2SiO_4$ composition (Zha et al. 1996) are also shown for comparison purposes. Error bars for the experimental data are smaller than the symbol size.

states (Fig. 6). These calculations show that the lowest energy excitation across the gap lies within the *d*-orbital manifold. While the top of the valence band also has slight oxygen character, the bulk of the oxygen *p*- and s-states lie at lower energy.

In order to understand the strong influence of U at high pressure, we have examined the influence of compression on magnetic structure (Fig. 7). We find that iron in both iron sites is in a high-spin state at ambient pressure. The calculated spin magnetic moments are 3.53 μ_B (Fe1) and 3.65 μ_B, (Fe2) with the GGA. For the GGA + U method, the values are 3.64 μ_B (Fe1) and 3.69 μ_B (Fe2) with $U = 2.0$ eV and 3.75 μ_B (Fe1) and 3.77 μ_B (Fe2) with $U = 4.8$ eV. The magnetic moments on the different iron sites become more similar with increasing values of U used. Our values are nearly identical to those obtained in previous studies that assumed an antiferromagnetic arrangement (Cococcioni et al., 2003; Jiang and Guo, 2004; Cococcioni and de Gironcoli, 2005), although slightly lower than the experimental value of 4.4 μ_B. The difference between theoretical and experimental values of the magnetic moment may be due to the assumption in this and previous studies of a co-linear spin arrangement whereas experimentally the spins are known to be non-co-linear. In the case of the GGA the magnetic moments remain nearly constant up to 10 GPa and then begin to decrease with increasing pressure. The decrease is pronounced, ending in partial magnetic collapse at the highest pressure studied (not shown). Upon reaching 32.3 GPa (Volume = 245.000 Å^3) the magnetic symmetry is broken and the moments on two of the four irons in Fe2 sites collapse, while the remaining Fe2 moments and all of the Fe1 moments retain finite values. In contrast, using the GGA + U method, the decrease in magnetic moment is very small with both U values, up to the highest pressure studied.

Numerical values for all results are included as supplementary material.

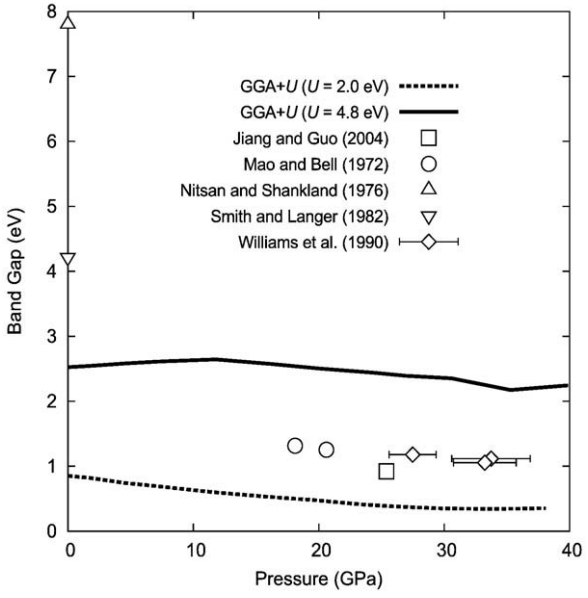

Fig. 5. Electronic band gap of fayalite as a function of pressure, calculated using the GGA + U method, with $U = 2.0$ eV and 4.8 eV, and corresponding experimental data.

4. Discussion

The addition of local Coulomb interactions significantly improves agreement between theory and experimental measurements of the band gap, crystal structure, equation-of-state, and elastic constants. This success is significant because it means that the GGA + U method, originally motivated by the tendency of density functional theory to under-predict the band gap, improves other physical properties as well. The degree of improvement is not large and this is consistent with previous studies of transition metal oxide systems using standard density functional theory, which have often found reasonable agreement with experiment, even though it wrongly predicts the band structure (Isaak et al., 1993a; Alfredsson et al., 2004). This suggests some cancellation of errors in density functional theory. While agreement with experimental data is reasonably good for our GGA + U calculations, in particular with $U = 2.0$ eV, it is not as good as found in previous studies of transition metal free systems with standard density functional theory (Oganov et al. 2001; Karki et al., 2001). This suggests that GGA + U, while an important improvement, does not fully capture the relevant physics of strongly correlated systems such as fayalite. The mixed success of the GGA + U method in describing the different properties of faylalite points to the importance of continued development of more exact methods such as Quantum Monte Carlo (Foulkes et al. 2001) in studies of iron-bearing insulators, which, at present, are applicable only to much simpler systems (Kolorenc and Mitas, 2008).

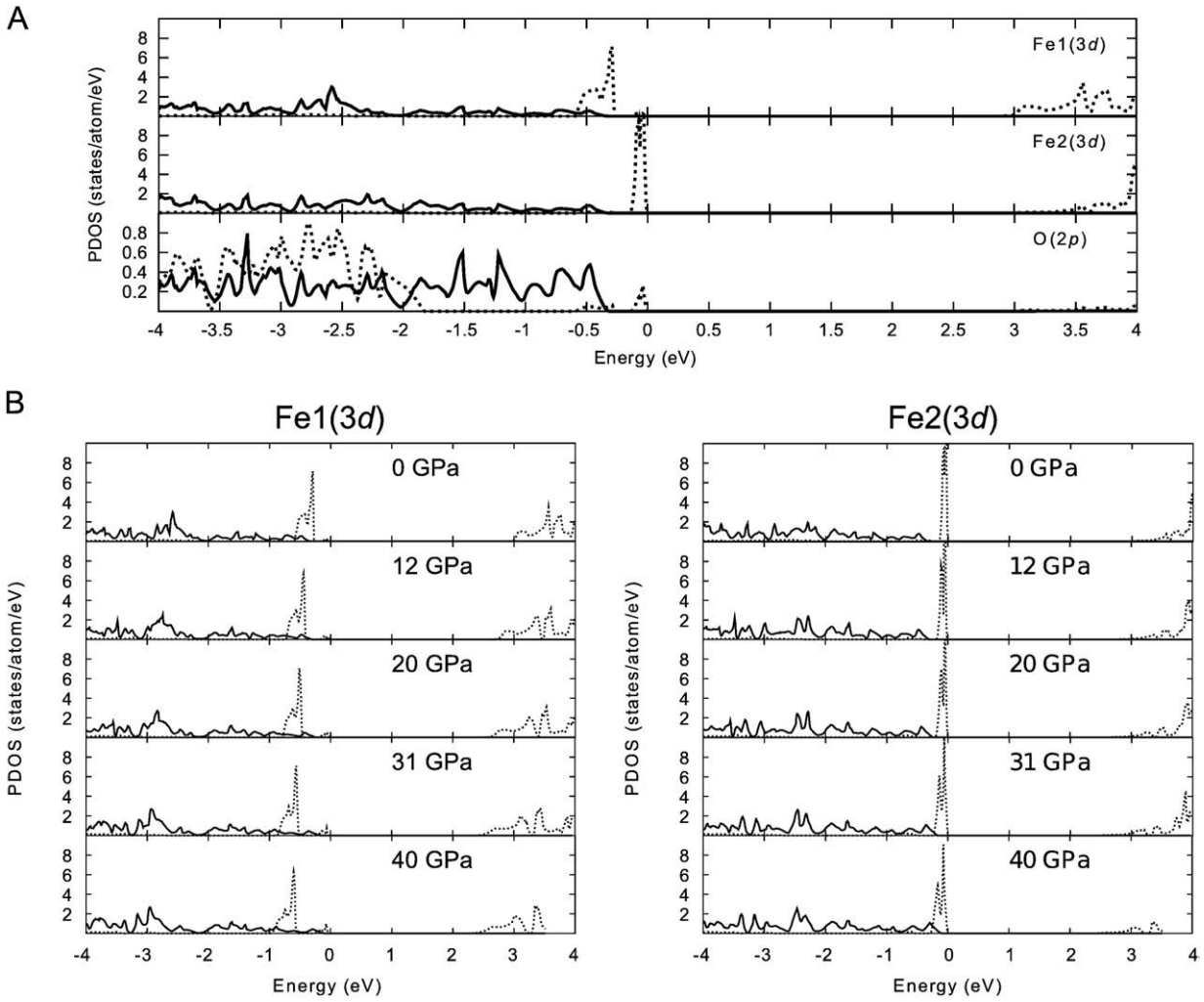

Fig. 6. Calculated partial density-of-states using the GGA + U method, with $U = 4.8$ eV. A: Partial density-of-states for Fe1($3d$), Fe2($3d$) and O($2p$) at ambient pressure. B: Partial density-of-states for Fe1($3d$) and Fe2($3d$) as a function of increasing pressure. The solid and dashed lines differentiate respectively the spin-up and spin-down components for Fe1($3d$) and Fe2($3d$).

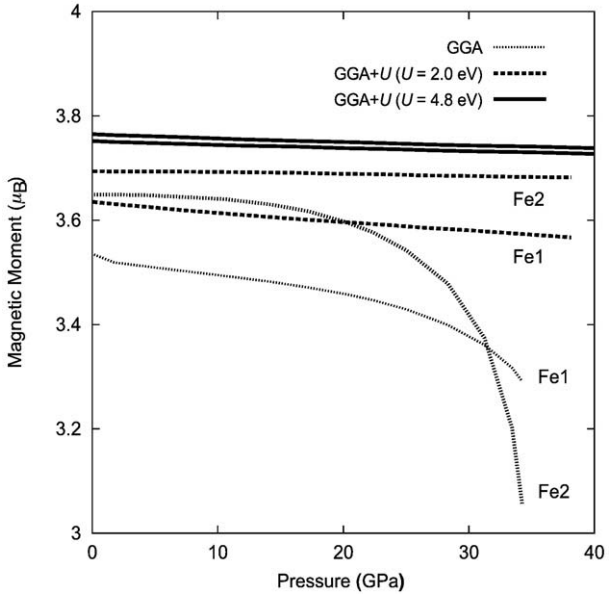

Fig. 7. Magnetic moment of the two iron sites in fayalite calculated using the GGA and GGA + U method, with $U = 2.0$ eV or 4.8 eV. In the GGA calculations, two out of the four iron atoms in site 2 underwent a spin transition to a low-spin state upon compression beyond the highest pressure shown.

The improvement in predicted elastic properties upon the addition of the local Coulomb repulsion calls for a re-examination of the predicted elastic properties of major mantle iron-bearing species. To date, these predictions have been based on standard density functional theory, without U, which the present results suggest could be in significant error. Predictions based on density functional theory form an important part of our understanding of the structure of the upper and lower mantle (Stixrude and Lithgow-Bertelloni, 2005; Stackhouse and Brodholt, 2008). In particular, the properties of iron-bearing phases are particularly critical in arguments concerning the non-thermal origin of deep mantle heterogeneity, for which lateral variations in iron-content have been proposed (Kiefer et al., 2002; Trampert et al., 2004; Brodholt et al., 2007). Our results, indicate that the GGA strongly underestimates the shear modulus of fayalite at high pressure (Fig. 4), which would lead to an underestimation of the amount of iron in the upper mantle.

The calculated elastic instability in fayalite is most likely to be the origin of experimentally observed pressure-induced amorphization (Williams et al., 1990; Richard and Richet, 1990; Andrault et al., 1995). The pressure at which c_{44} vanishes in our GGA + U calculations, with $U = 2.0$ eV, coincides with that of a sudden reduction in the amplitude of X-ray diffraction peaks in diamond anvil cell experiments. The vanishing of c_{44} means that fayalite violates one of the Born stability criteria and cannot be preserved even in a metastable state. It must spontaneously transform to a new structural state. This state need not be one of thermodynamic equilibrium. Indeed a simple shear cannot

transform fayalite to the stable assemblage of wüstite and stishovite at 40 GPa. It is plausible that the mismatch between the un-restored shear associated with vanishing c_{44} and the stable thermodynamic state produces frustration that leads to amorphization. Pressure-induced amorphization has been associated with unstable phonon modes in other systems (Wentzcovitch et al., 1998).

The influence of iron on the shear modulus is stronger at high pressure than at low pressure (Fig. 4). The addition of iron to mantle silicates and oxides reduces the shear-wave velocity by increasing the density and decreasing the shear modulus. We find that the shear modulus of fayalite depends much less strongly on pressure than that of forsterite. This causes the shear moduli of the two end-members to diverge on compression. The effect of iron on the seismic properties of olivine will be particularly large near the bottom of a metastable olivine wedge.

We argue that the band gap in fayalite at ambient pressure is closer to our theoretical prediction of between 0.85 eV ($U=2.0$ eV) and 2.52 eV ($U=4.8$ eV) than previous experimental measurements of the optical absorption edge (Mao and Bell, 1972; Nitsan and Shankland, 1976; Smith and Langer, 1982). We suggest that the fundamental gap is not observed at ambient pressure because the signal in the optical spectrum is too weak. We find that the fundamental gap involves a transition from Fe2($3d$) in the valence band to Fe1($3d$) in the conduction band (Fig. 6). This transition is dipole forbidden and likely to have very small amplitude (Jiang and Guo, 2004). In contrast, the higher energy transitions from O($2p$) in the valence band to Fe1($3d$) in the conduction band, which have the greatest intensity above 4 eV (Jiang and Guo, 2004) will have a much larger amplitude, and this is likely the lowest energy peak that was observed in optical spectra.

The nature of the gap changes at high pressure due to the broadening of the $3d$ manifold: Fe1($3d$) states become more prominent at the valence band maximum, and Fe2($3d$) states become more prominent at the conduction band minimum (Fig. 6). These changes in the electronic structure likely render the fundamental gap observable in optical spectroscopy at high pressure, accounting for the reasonable agreement between theory and experiment above 20 GPa (Fig. 5).

Pressure-induced changes in the character of the bands are associated with a change in the crystal structure. We find that at high pressure, the chains of M1 octahedra straighten out so that Fe–Fe pairs are nearly co-planar with the shared octahedral edge (Fig. 8). This change in the crystal structure will lead to increased Fe–Fe bonding, accounting for the broadening of the Fe($3d$) band. Fe–Fe interactions across shared octahedral edges have also been invoked to explain the observed rhombohedral distortion in wüstite (Isaak et al., 1993a).

Magnetic collapse appears not to take place in fayalite prior to the mechanical instability near 40 GPa. While the GGA predicts partial magnetic collapse, the GGA $+U$ results show full magnetic moments up to the elastic instability. The effect of U is expected: the local Coulomb repulsion strengthens correlation, making spin pairing less favorable and tending to inhibit magnetic collapse. Experimental measurements of the magnetic moments in fayalite have not yet been performed at high pressure. However the excellent agreement between the GGA $+U$ calculations and experiment and the poor agreement between the GGA and experiment in the pressure regime of the GGA magnetic collapse, indicates that the GGA $+U$ method provides the more accurate picture.

It is interesting to note that although we presume the GGA results are inaccurate, they reveal an aspect of magnetic collapse that may be observable in other iron-bearing oxides and silicates: the two symmetrically inequivalent iron atoms behave differently, with one showing more rapid magnetic collapse than the other upon compression. The situation is quite different from heterovalent compounds, such as iron-bearing $MgSiO_3$ perovskite which may contain both ferrous and ferric iron. High-to-low-spin transitions of two or more symmetrically inequivalent ferrous iron ions have not yet been observed in oxides or silicates at high pressure. The distinct character of iron on the two sites in fayalite is also highlighted by the nature of magnetic transitions at temperatures below the Néel temperature (Aronson et al., 2007), and the magnetic properties of pressure-amorphized fayalite glass (Kruger et al., 1992).

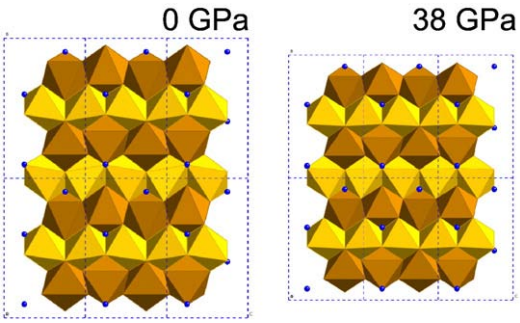

Fig. 8. Observed change in the crystal structure of fayalite upon compression. Iron in site 1 is yellow, iron in site 2 is brown, silicon is blue and oxygen is not shown. One can see that the ribbons formed by edge-sharing iron in site 1 become straighter upon compression, leading to increased Fe–Fe interaction.

5. Conclusions

Theoretical prediction of the properties of transition metal bearing insulators remains a fundamental challenge in condensed matter physics. Many of the new techniques that have been developed to study them are still far too expensive and cumbersome to treat even relatively simple crystal structures, like fayalite. Our results show that the GGA $+U$ method is a valuable tool for exploring such systems and is much more accurate than the GGA alone, even though the accuracy is still not as high as in studies of transition-metal-free mantle phases with standard density functional theory. This calls for a re-examination of the elastic properties of iron-bearing phases determined with standard density functional theory methods, ($U=0$ eV), which could be inaccurate, leading to inaccurate estimates of the concentration of iron in mantle phases.

Our results show a range of interesting phenomenon in fayalite upon compression, including narrowing, but not closing of the band gap on compression, broadening of the d-bands that likely produce changes in experimentally observed optical spectra, and an elastic instability that may be the cause of amorphization in the phase.

The change in electronic structure is known to be associated with an increase in the conductivity of fayalite on compression (Williams et al., 1990), that is likely to be important in understanding geophysical observations of mantle electrical conductivity (Toffelmier and Tyburczy, 2007). Our result suggest that olivine is not likely to amorphize in a subducting slab, even taking into account the possible influence of non-hydrostatic stress (Wu et al., 1993), as fayalite amorphizes at pressures well beyond the extent of the proposed metastable wedge (Green and Burnley, 1989), and experimental results show that increasing the forsterite component raises the pressure at which amorphization occurs (Andrault et al., 1995).

Acknowledgement

The bulk of the calculations were performed at the Center for Advance Computing at the University of Michigan and HECToR, the U.K. national high-performance computing service. In addition, some of the initial calculations were carried out on a Linux cluster belonging to the group of Todd Ehlers at the Department of Geological Sciences at the University of Michigan. The work supported by the U. K. National Environmental Research Council, and the U. S. National Science Foundation under grant number EAR-0635815.

Appendix A. Supplementary data

Supplementary data associated with this article can be found, in the online version, at doi:10.1016/j.epsl.2009.11.033.

References

Alfredsson, M., Price, G.D., Catlow, C.R.A., Parker, S.C., Orlando, R., Brodholt, J.P., 2004. Electronic structure of the antiferromagnetic *B*1-structured FeO. Phys. Rev., B 70, 165111.

Anderson, O.L., Isaak, D.G., 1995. Elastic constants of mantle minerals at high temperature. In: Ahrens, T.J. (Ed.), Mineral Physics and Crystallography: A Handbook of Physical Constants. Am. Geophys. Union, Washington D.C., pp. 64–97.

Andrault, D., Bouhifd, M.A., Itié, J.P., Richet, P., 1995. Compression and amorphization of $(Mg, Fe)_2SiO_4$ olivines: An X-ray diffraction study up to 70 GPa. Phys. Chem. Miner. 22, 99–107.

Anisimov, V.I., Zaanen, J., Andersen, O.K., 1991. Band theory and Mott insulators: Hubbard U instead of Stoner I. Phys. Rev., B 44, 943–954.

Anisimov, V.I., Aryasetiawan, F., Lichtenstein, A.I., 1997. First-principles calculations of the electronic structure and spectra of strongly correlated systems: the LDA+ *U* method. J. Phys., Condens. Matter 9, 767–808.

Aronson, M.C., Stixrude, L., David, M.K., Gannon, W., Ahilan, K., 2007. Magnetic excitations and heat capacity of fayalite Fe_2SiO_4. Am. Mineral. 92, 481–490.

Badro, J., Rueff, J.P., Vanko, G., Monaco, G., Fiquet, G., Guyot, F., 2004. Electronic transitions in perovskite: Possible nonconvecting layers in the lower mantle. Science 305, 383–386.

Bengtson, A.K., Persson, K., Morgan, D., 2008. Ab initio study of the composition dependence of the pressure-induced spin crossover in perovskite (Mg1-x, Fex)SiO3. Earth Planet. Sci. Lett. 265, 535–545.

Birch, F., 1947. Finite elastic strain of cubic crystals. Phys. Rev. 71, 809–824.

Blöchl, P.E., 1994. Projector augmented-wave method. Phys. Rev., B 50, 17953–17979.

Blöchl, P.E., Jepsen, O., Andersen, O.K., 1994. Improved tetrahedron method for Brillouin-zone integrations. Phys. Rev., B 49, 16223–16233.

Brodholt, J.P., Vočadlo, L., 2006. Applications of density functional theory in the geosciences. MRS Bull. 31, 675–680.

Brodholt, J.P., Helffrich, G., Trampert, J., 2007. Chemical versus thermal heterogeneity in the lower mantle: The most likely role of anelasticity. Earth Planet. Sci. Lett. 262, 429–437.

Caracas, R., Cohen, R.E., 2005. Effect of chemistry on the stability and elasticity of the perovskite and post-perovskite phases in the $MgSiO_3$–$FeSiO_3$–Al_2O_3 system and implications for the lowermost mantle. Geophys. Res. Lett. 32, L16310.

Cococcioni, M., de Gironcoli, S., 2005. Linear response approach to the calculation of the effective interaction parameters in the LDA+U method. Phys. Rev., B 71, 035105.

Cococcioni, M., Dal Corso, A., de Gironcoli, S., 2003. Structural, electronic and magnetic properties of Fe_2SiO_4 fayalite: Comparison of LDA and GGA results. Phys. Rev., B 67, 094106.

de Koker, N.P., Stixrude, L., Karki, B.B., 2008. Thermodynamics, structure, dynamics and freezing of Mg_2SiO_4 liquid at high pressures. Geochim. Cosmochim. Acta 72, 1427–1441.

Dudarev, S.L., Botton, G.A., Savrasov, S.Y., Humphreys, C.J., Sutton, A.P., 1998. Electron-energy-loss spectra and the structural stability of nickel oxide: an LSAD+U study. Phys. Rev. 57, 1505–1509.

Foulkes, W.M.C., Mitas, L., Needs, R.J., Rajagopal, G., 2001. Quantum Monte Carlo simulations of solids. Rev. Mod. Phys. 73, 33–83.

Fujino, K., Sasaki, S., Takéuchi, Y., Sadanaga, R., 1980. X-ray determination of electron distributions in forsterite, fayalite and tephroite. Acta Crystallogr., B 37, 513–518.

Graham, E.K., Schwab, J.A., Sopkin, S.M., Takei, H., 1988. The pressure and temperature dependence of the elastic properties of single-crystal fayalite Fe_2SiO_4. Phys. Chem. Miner. 16, 186–198.

Gramsch, S., Cohen, R.E., Savrasov, S.Y., 2003. Structure, metal-insulator transitions, and magnetic properties of FeO at high pressure. Am. Mineral. 88, 257–261.

Green II, H.W., Burnley, P.C., 1989. A new self-organizing mechanism for deep-focus earthquakes. Nature 341, 733–737.

Hayashi, M., Tamura, I., Shimomura, O., Sawamoto, H., Kawamura, H., 1987. Antiferromagnetic transition of fayalite under high pressure studied by Mössbauer spectroscopy. Phys. Chem. Miner. 14, 241–344.

Hill, R., 1963. Elastic properties of reinforced solids: Some theoretical principles. J. Mech. Phys. Solids 11, 357–372.

Hohenberg, P., Kohn, W., 1964. Inhomogeneous electron gas. Phys. Rev. 136, B864–B871.

Isaak, D.G., Cohen, R.E., Mehl, M.J., Singh, D.J., 1993a. Phase stability of wüstite at high pressure from first-principles linearized augmented plane-wave calculations. Phys. Rev., B 47, 7720–7731.

Isaak, D.G., Graham, E.K., Bass, J.D., Wang, H., 1993b. The elastic properties of single-crystal fayalite as determined by dynamical measurement techniques. Pure Appl. Geophys. 141, 393–414.

Jiang, X., Guo, G.Y., 2004. Electronic structure, magnetism, and optical properties of Fe_2SiO_4 fayalite at ambient and high pressures: A GGA+U study. Phys. Rev., B 69, 155108.

Karki, B.B., Stixrude, L., Wentzcovitch, R.M., 2001. High-pressure elastic properties of major materials of Earth's mantle from first principles. Rev. Geophys. 39, 507–534.

Kiefer, B., Stixrude, L., Wentzcovitch, R.M., 2002. Elasticity of $(Mg, Fe)SiO_3$-perovskite at high pressures. Geophys. Res. Lett. 29, L014683. doi:10.1029/2002GL014683.

Kingma, K.J., Meade, C., Hemley, R.J., Mao, H.-K., Veblen, D.R., 1993. Microstructural observations of alpha-quartz amorphization. Science 259, 666–669.

Kohn, W., Sham, L.J., 1965. Self-consistent equations including exchange and correlation effects. Phys. Rev. 140, A1133–A1138.

Kolorenc, J., Mitas, J., 2008. Quantum Monte Carlo calculations of structural properties of FeO under pressure. Phys. Rev. Lett. 101, 185502.

Kresse, G., Furthmüller, J., 1996a. Efficient iterative schemes for ab initio total-energy calculations using a plane-wave basis set. Phys. Rev., B 54, 11169–11186.

Kresse, G., Furthmüller, J., 1996b. Efficiency of ab initio total energy calculations for metals and semiconductors using a plane-wave basis set. Comput. Mater. Sci. 6, 15–50.

Kresse, G., Joubert, D., 1999. From ultrasoft pseudopotentials to the projector augmented-wave method. Phys. Rev., B 59, 1758–1775.

Kruger, M.B., Jeanloz, R., Pasternak, M.P., Taylor, R.D., Snyder, B.S., Stacy, A.M., Bohlen, S.R., 1992. Antiferromagnetism in pressure-amorphized Fe_2SiO_4. Science 255, 703–705.

Kudoh, Y., Takeda, H., 1986. Single crystal X-ray diffraction study on the bond compressibility of fayalite, Fe_2SiO_4 and rutile, TiO_2 under high pressure. Physica 139B, 333–336.

Li, L., Brodholt, J.P., Stackhouse, S., Weidner, D., Alfredsson, M., Price, G.D., 2005. Elasticity of $(Mg, Fe)(Si, Al)O_3$-perovskite at high pressure. Earth Planet. Sci. Lett. 240, 529–536.

Mao, H.K., Bell, P.M., 1972. Electrical conductivity and the red shift of absorption in olivine and spinel at high pressure. Science 176, 403–405.

Mermin, D.M., 1965. Thermal properties of the inhomogeneous electron gas. Phys. Rev. 137, 1441–1443.

Monkhorst, H.J., Pack, J.D., 1976. Special points for Brillouin-zone integrations. Phys. Rev., B 13, 5188–5192.

Nitsan, U., Shankland, T.J., 1976. Optical properties and electronic structure of mantle silicates. Geophys. J. R. Astron. Soc. 45, 59–81.

Oganov, A.R., Brodholt, J.P., Price, G.D., 2001. Ab initio elasticity and thermal equation of state of $MgSiO_3$ perovskite. Earth Planet. Sci. Lett. 184, 555–560.

Perdew, J.P., Burke, K., Ernzerhof, M., 1996. Generalized gradient approximation made simple. Phys. Rev. Lett. 77, 3865–3868.

Richard, G., Richet, P., 1990. Room-temperature amorphization of fayalite and high-pressure properties of Fe_2SiO_4 liquid. Geophys. Res. Lett. 17, 2093–2096.

Richet, P., Gillet, P., 1997. Pressure-induced amorphization of minerals: A review. Eur. J. Mineral. 9, 907–933.

Ringwood, A.E., 1970. Phase transformations and the constitution of the mantle. Phys. Earth Planet. Inter. 3, 109–155.

Smith, H.G., Langer, K., 1982. Single crystal spectra of olivines in the range 45,000–5,000 cm^{-1} at pressures up to 200 kbar. Am. Mineral. 67, 343–348.

Speziale, S., Duffy, T.S., Angel, R.J., 2004. Single-crystal elasticity of fayalite to 12 GPa. J. Geophys. Res. 109, B12202.

Stackhouse, S., Brodholt, J.P., 2008. Elastic properties of the post-perovskite phase of Fe_2O_3 and implications for ultra-low velocity zones. Phys. Earth Planet. Inter. 170, 260–266.

Stackhouse, S., Brodholt, J.P., Price, G.D., 2006. Elastic anisotropy of $FeSiO_3$ end-members of perovskite and post-perovskite phases. Geophys. Res. Lett. 33, L01304.

Stixrude, L., Lithgow-Bertelloni, C., 2005. Thermodynamics of mantle minerals — I. Physical properties. Geophys. J. Int. 162, 610–632.

Stixrude, L., Cohen, R.E., Hemley, R.J., 1998. Theory of minerals at high pressure. Rev. Miner. 37, 639–671.

Sumino, Y., 1979. The elastic constants of Mn_2SiO_4, Fe_2SiO_4, and Co_2SiO_4 and the elastic properties of olivine group minerals at high temperature. J. Phys. Earth 27, 209–238.

Toffelmier, D.A., Tyburczy, J.A., 2007. Electromagnetic detection of a 410-km-deep melt layer in the southwestern United States. Nature 447, 991–994.

Trampert, J., Deschamps, F., Resovsky, J., Yuen, D., 2004. Probabilistic tomography maps chemical heterogeneities throughout the lower mantle. Science 306, 853–856.

Tsuchiya, T., Tsuchiya, J., 2006. Effect of impurity on the elasticity of perovskite and postperovskite: Velocity contrast across the postperovskite transition in $(Mg,Fe,Al)(Si,Al)O_3$. Geophys. Res. Lett. 33, L12S04.

Umemoto, K., Wentzcovitch, R.M., Allen, P.B., 2006. Dissociation of $MgSiO_3$ in the cores of gas giants and terrestrial exoplanets. Science 311, 983–986.

Wang, J., Bass, J.D., Rossman, G.R., 1989. Elastic properties of Fe-bearing pyroxenes and olivines (abstract). Eos Trans. AGU 70, 474.

Wentzcovitch, R.M., da Silva, C., Chelikowsky, J.R., Binggeli, N., 1998. A new phase and pressure induced amorphization in silica. Phys. Rev. Lett. 80, 2149–2152.

Williams, Q., Knittle, E., Reichlin, R., Martin, S., Jeanloz, R., 1990. Structural and electronic properties of Fe_2SiO_4-fayalite at ultrahigh pressures: Amorphization and gap closure. J. Geophys. Res. 95, 21549–21563.

Wu, T.-C., Basset, W.A., Burnley, P.C., Weathers, M.S., 1993. Shear-promoted phase transitions in Fe_2SiO_4 and Mg_2SiO_4 and the mechanism of deep earthquakes. J. Geophys. Res. 98, 19767–19776.

Xu, W., Lithgow-Bertelloni, C., Stixrude, L., Ritsema, J., 2008. The effect of bulk composition and temperature on mantle seismic structure. Earth Planet. Sci. Lett. 275, 70–79.

Yagi, T., Akaogi, M., Shimomura, O., Suzuki, T., Akimoto, S., 1987. In situ observation of the olivine-spinel phase-transformation in Fe_2SiO_4 using synchrotron radiation. J. Geophys. Res. B7, 6207–6213.

Zha, C.-S., Duffy, T.S., Downs, R.T., Mao, H.-K., Hemley, R.J., 1996. Sound velocity and elasticity of single-crystal forsterite to 16 GPa. J. Geophys. Res. 101, 17535–17545.

Zhang, L., 1998. Single crystal hydrostatic compression of $(Mg, Mn, Fe, Co)_2SiO_4$ olivines. Phys. Chem. Miner. 25, 308–312.